CrystEngComm

COMMUNICATION

View Article Online
View Journal | View Issue

Check for updates

Cite this: *CrystEngComm*, 2019, **21**, 1358

Received 20th December 2018,
Accepted 1st February 2019

DOI: 10.1039/c8ce02153h

rsc.li/crystengcomm

Microwave-assisted synthesis of urea-containing zirconium metal–organic frameworks for heterogeneous catalysis of Henry reactions†

He Zhang,[a] Xue-Wang Gao,[b] Li Wang,[a] Xinsheng Zhao,[a]
Qiu-Yan Li *[a] and Xiao-Jun Wang *[abc]

Here we report the facile preparation of a urea-containing UiO-68 isoreticular zirconium metal–organic framework (MOF) with mixed dicarboxylate struts by utilizing a microwave-assisted heating method. It can work as an efficient hydrogen-bond-donating heterogeneous catalyst for Henry reactions of benzaldehydes and nitroalkanes. This mixed strut MOF exhibits improved catalytic activity compared to the pure urea-functionalized linker based analogue.

Organic reactions through hydrogen-bond catalytic processes have emerged as a useful synthetic method and gained much intense research interest over the past years.[1–4] These hydrogen-bond-donating (HBD) catalysts usually utilize urea or thiourea as the key functional moiety on account of two-point hydrogen bonding *via* acidic N–H protons.[1–7] A variety of bond-forming transformations, such as Diels–Alder and Friedel–Crafts (FC) reactions,[8,9] have been catalyzed by HBD species in the solution phase, often along with good to excellent selectivity and yield. However, these HBD catalysts, in particular urea derivatives, would suffer from the self-quenching problem in a homogeneous catalysis system, due to their high propensity of dimerization and oligomerization *via* H-bonding interactions of catalyst molecules to each other.[10–14] This undesirable self-association behavior greatly lowers the catalyst's solubility, resulting in the potential decrease of its catalytic reactivity.

Consequently, the immobilization of HBD organocatalysts into solid architectures in which H-bonding donor sites are physically separated to prevent their detrimental self-quenching is a promising and practical strategy to promote catalyst-substrate recognition for improving the catalytic activity.[15] For example, Portnoy and Tuchman-Shukron have incorporated H-bond donors into polystyrene for the asymmetric nitro-Michael reaction of acetone to nitro-olefins with high enantioselectivity.[16] Borah *et al.* recently prepared a urea-pyridine-bridged periodic mesoporous organosilica (PMO) that exhibited a high catalytic efficacy for the Henry reaction.[17] Farha and his coworkers first engineered HBD catalysis into a metal–organic framework (MOF) material for FC reaction of pyrroles and nitroalkenes, achieving an increased rate enhancement *versus* its homogeneous urea-counterpart due to the spatial isolation of catalytic centers in MOF scaffolds.[18]

Among these materials for anchoring HBD catalysts, MOFs as a family of hybrid porous materials that are constructed from inorganic nodes coordinated with polytopic organic struts possess several unique advantages, including high surface area along with tunable pore size as well as structural diversity and tailorability.[19–34] These fascinating features of MOFs enable them to act as a highly versatile platform in this regard. As a result, continuous effort has been made to fabricate more HBD organocatalyst based MOFs to evaluate and optimize their performance in recent years.[35–47] However, the wide and practical application of these catalysts is still impeded by some challenges, such as poor stabilities of MOFs during catalysis, as well as unsatisfactory yields and limited substrate scopes. Besides, the conventional solvothermal reaction for preparing MOF materials is time-consuming and inefficient. In contrast, microwave irradiation that can quickly heat reactants to high temperature and enable a fast nucleation rate, while reducing the reaction time and promoting the conversion rate, has emerged as a very promising technique for MOF production.[48–51]

It has been well recognized that high-valent Zr(IV)-based MOFs exhibited an outstanding stability in contrast to

---

[a] *Jiangsu Key Laboratory of Green Synthetic Chemistry for Functional Materials, School of Chemistry and Materials Science, and School of Physics and Electronic Engineering, Jiangsu Normal University, Xuzhou 221116, P. R. China. E-mail: qyli@jsnu.edu.cn, xjwang@jsnu.edu.cn*

[b] *Key Laboratory of Photochemical Conversion and Optoelectronic Materials, Technical Institute of Physics and Chemistry, Chinese Academy of Sciences, Beijing 100190, P. R. China*

[c] *Department of Chemistry and Key Laboratory for Preparation and Application of Ordered Structural Materials of Guangdong Province, Shantou University, Guangdong 515063, P. R. China*

† Electronic supplementary information (ESI) available: Experimental procedure, additional synthesis and characterization data. CCDC 1889711. For ESI and crystallographic data in CIF or other electronic format see DOI: 10.1039/c8ce02153h

divalent metal ions analogues, such as Zn^{2+} and Cu^{2+}.[52,53] UiO series MOFs (UiO stands for University of Oslo), including UiO-66, UiO-67, and UiO-68 with an isostructural framework based on the same secondary building unit $[Zr_6(\mu_3\text{-}O)_4(\mu_3\text{-}OH)_4(COO)_{12}]$ but different dicarboxylate linker lengths, should be the most representative one among the stable Zr-MOF materials.[54,55] Recently, Hupp, Farha and their coworkers have utilized the UiO-67 framework for the incorporation of self-associative urea and squaramide moieties to "turn on" their HBD catalysis.[37,41] However, it would be difficult to accept large substrates in these UiO-67 derivatives composed of biphenyl-4,4′-dicarboxylate struts. With these concerns, we here report the rapid synthesis of a urea-containing UiO-68 isoreticular MOF with two mixed terphenyldicarboxylate (TPDC) struts by the microwave-assisted heating method (Scheme 1). Its efficacy serving as a HBD catalyst was subsequently exemplified through Henry reactions of benzaldehydes and nitroalkanes. The large pores or cavities in the UiO-68 framework will facilitate the transport of catalytic substrates and products in the framework, allowing a broad substrate scope.

The urea-containing TPDC derivative strut H_2-utpdc has been conveniently synthesized by several typical organic reactions as depicted in Scheme S1 (for details see the ESI†). Initially, we tried to prepare a pure urea strut functionalized MOF under microwave-assisted solvothermal conditions. However, we were unable to obtain a good crystalline UiO MOF even after variation of reaction conditions, presumably ascribing to the steric bulk of this organic linker. A mixed-strut approach was employed to introduce such a sterically demanding urea-functionalized moiety from the linker into the UiO-68 framework.[56–58] Because of the very limited solubility of the TPDC ligand in the original UiO-68 MOF, we utilized another MOF PCN-56 (PCN stands for porous coordination network) with the same UiO-68 type structure to act as the parent framework for accommodation of the urea moiety.[59] Specifically, a mixture of H_2-mtpdc and H_2-utpdc struts in a 1 : 1 molar ratio was reacted with $ZrCl_4$ by using HCl as a modulator in DMF at 120 °C under microwave irradiation for 1 h (Scheme 1), generating a highly crystalline UiO-68 derivative MOF material (denoted as PCN-56-UM). In comparison to the conventional solvothermal method for preparing UiO Zr-MOFs, which normally takes several days, this microwave assisted synthesis greatly reduced the reaction time.

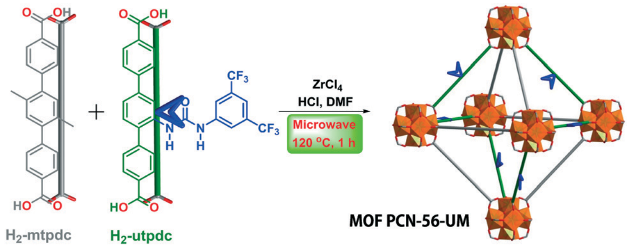

Scheme 1 Rapid preparation for the mixed strut MOF PCN-56-UM with TPDC linkers of 2′,5′-dimethyl-[1,1′:4′,1″-terphenyl]-4,4″-dicarboxylic acid (denoted as H_2-mtpdc) and 2′-(3-(3,5-bis(trifluoromethyl)phenyl)ureido)-[1,1′:4′,1″-terphenyl]-4,4″-dicarboxylic acid (denoted as H_2-utpdc) *via* a microwave method.

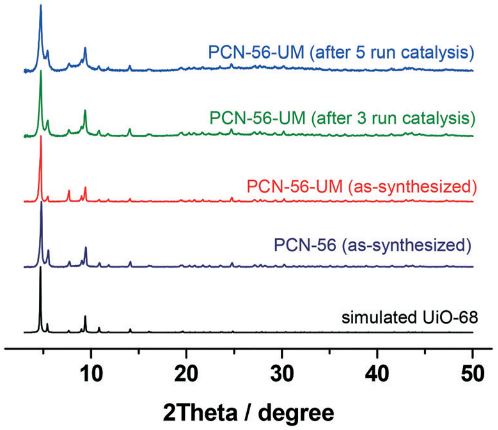

Fig. 1 Powder X-ray diffraction (PXRD) patterns of simulated UiO-68, PCN-56, mixed strut PCN-56-UM and post-catalysis PCN-56-UM.

In contrast to the pure urea-functionalized strut PCN-56-U, powder X-ray diffraction (PXRD) of mixed strut PCN-56-UM reveals its highly crystalline nature with well-resolved and sharp peaks (Fig. 1). And its PXRD pattern nicely matches with that of PCN-56, confirming its isostructural UiO-68 framework. Additionally, nitrogen sorption measurements of these MOF materials at 77 K exhibit typical type I reversible isotherms but with different Brunauer–Emmett–Teller (BET) surface areas of 3504, 2594 and 290 $m^2\ g^{-1}$ for PCN-56, PCN-56-UM and PCN-56-U, respectively (Fig. 2). The large decrease of the BET surface area for PCN-56-UM, relative to parent MOF PCN-56, should be attributed to the successful incorporation of the urea motif into the UiO-68 framework. While there is no remarkable difference between their pore size distributions (~1.6 nm) calculated by nonlocal density functional theory (Fig. S3†), this implies that the relatively large urea-functionalized moiety of the H_2-utpdc linker should be homogeneously distributed within the whole framework of PCN-56-UM. Besides, the scanning electron microscopy

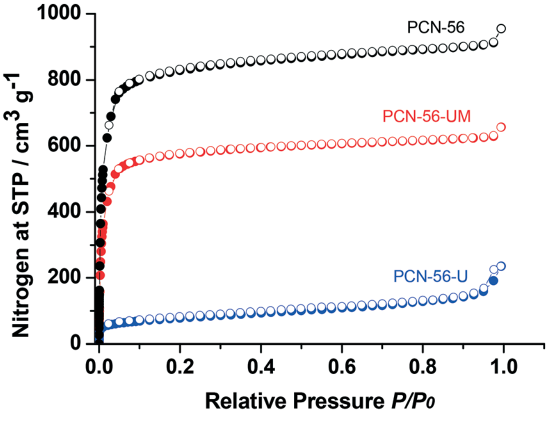

Fig. 2 N_2 isotherms of PCN-56, PCN-56-UM and PCN-56-U at 77 K. The filled and open circles represent adsorption and desorption, respectively.

elemental mapping experiment for the PCN-56-UM sample was performed as depicted in Fig. S4 (ESI†). It was found that the fluorine element from the H_2-uptdc ligand matches well with other elements, indicative of the single phase instead of mixed PCN-56 and PCN-56-U phases. In contrast, the elemental mapping image of the physical mixture revealed the distinct phase separation in both morphology and elemental distribution, as indicated by the uneven fluorine distribution (Fig. S5†).[60]

The pores or channels in the PCN-56-UM architecture remained open during this microwave-assisted mixed-strut synthetic process, thus, facilitating the diffusion of substrates and products into and out of the framework for efficient heterogeneous catalysis. Furthermore, the MOF was digested by HF in DMSO and analyzed by ^{1}H NMR spectroscopy (Fig. S6 in the ESI†). We can clearly observe two types of proton signal peaks corresponding to two struts H_2-mtpdc and H_2-utpdc with a molar ratio of 1.08 : 1 in the framework. The slightly higher content of H_2-mtpdc should be ascribed to the steric bulk of the H_2-utpdc linker. Besides, no decomposition of organic linkers was detected in ^{1}H NMR of digested PCN-56-UM. It suggests that this microwave-assisted MOF preparation is a mild reaction that did not destroy the catalytically active urea site.

Considering the high surface area and large open channel as well as the intact urea moiety in the PCN-56-UM framework, we utilized the Henry reaction of *p*-tolualdehyde and nitromethane as a model reaction to evaluate its HBD catalytic ability. As shown in Fig. 3, the reaction with 5 mol% catalyst loading of PCN-56-UM was performed in THF at room temperature and the progress was monitored by using ^{1}H NMR method. As expected, the desired 2-nitroalkanol product can be obtained in a high yield of 90% after 24 h. And no remarkable increase was detected with further extending the reaction time. While only 14% yield was obtained by using parent MOF PCN-56 without the urea strut as a control catalyst under the same conditions, this validates that the urea moiety in the mixed strut PCN-56-UM framework can work as an effective HBD catalyst site. Besides, the reaction catalyzed by UiO-67 derivative MOF UiO-67-Urea/bpdc with smaller pore size gave a lower yield of 65% after 24 h in comparison to that of PCN-56-UM (Table S1 in the ESI†). This confirmed that the large open channels in PCN-56-UM should promote the substrate and product in and out of the framework, thus, enhancing the catalytic activity.

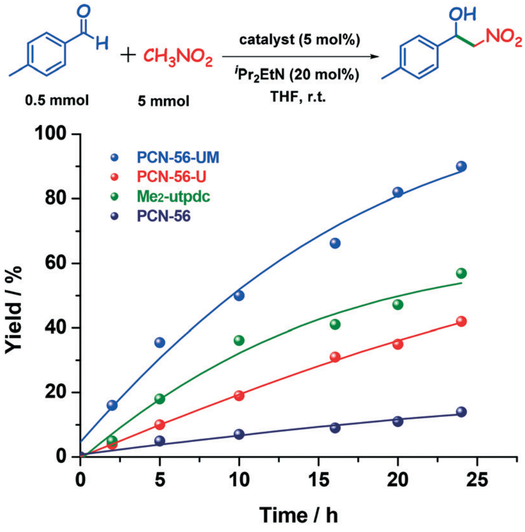

Fig. 3 Catalytic profiles of the mixed strut PCN-56-UM, pure strut PCN-56-U and Me_2-utpdc for the Henry reaction of *p*-tolualdehyde and nitromethane in THF. The control reaction was performed by using urea-free PCN-56 as a catalyst. The reaction progress was monitored by ^{1}H NMR.

Because of the better solubility of the diester precursor in comparison to the H_2-utpdc linker, we employed Me_2-utpdc as a homogenous HBD catalyst to perform the reaction, giving a moderate catalytic activity but lower than that of PCN-56-UM (56% yield at 24 h *vs.* 90% yield). This should be ascribed to the hydrogen bonding between urea N–H and C═O of ester (Fig. S9 in the ESI†). While the incorporation of the urea strut into the MOF framework will eliminate this hydrogen bonding through spatial isolation, thus, leading to enhanced catalytic activity. Additionally, it was found that pure urea strut functionalized MOF PCN-56-U exhibited a lower catalytic activity (41% at 24 h, Fig. 3). The low yield may be caused by the shrinking of pores and collapse of the framework of the MOF (BET 290 $m^2\ g^{-1}$ in Fig. 2). This will greatly limit the diffusion of the substrate and accessibility of the catalytic urea site in the framework as well as limit the catalysis mainly occurring on its external surface. Furthermore, we sufficiently ground these two MOF samples and repeated the catalytic reaction, resulting in 39% and 50% yields for PCN-56-U and PCN-56-UM, respectively. The large decrease of the catalytic yield from 90% to 50% for PCN-56-UM before and after grinding should be attributed to the induced partial collapse and blocking of pores on the external surface, which makes the catalytic reaction mainly occur on the outer surface. In contrast, the decrease is negligible for the case of PCN-56-U. Additionally, when PCN-56 was utilized in conjunction with the pure urea strut PCN-56-U (1 : 1 molar ratio) as catalysts, no synergistic effect in this physical mixture catalytic system was observed (29% yield at 24 h). These results indicated that the mixed-strut synthetic approach can allow PCN-56-UM to preserve the high porosity and open pores of the framework, which is critical to the catalytic activity of the urea moiety in the MOF scaffold.

The heterogeneous catalysis of PCN-56-UM was confirmed by catalyst filtration and recyclability. The MOF HBD catalyst was removed from the reaction mixture after 5 h (yield: 35%). And no significant increase of product was observed after another 12 h, indicative of the heterogeneity of MOF PCN-56-UM along with no leaching of catalytic species into solution during catalysis. Meanwhile, the reusability of PCN-56-UM was performed, which can be easily recovered from the reaction system *via* centrifugation. The same batch of PCN-56-UM for the catalytic reaction was successively obtained over five cycles only with a small loss of the catalytic activity (73%

Table 1 Mixed-strut MOF PCN-56-UM catalysed reactions of benzaldehydes with nitroalkanes and dimethyl malonate[a]

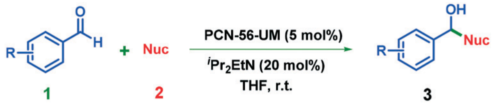

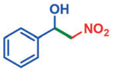 **3b** (89%)	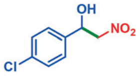 **3c** (86%)	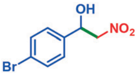 **3d** (87%)	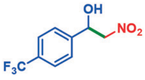 **3e** (90%)
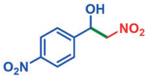 **3f** (93%)	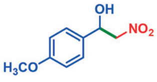 **3g** (62%)	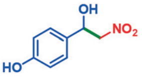 **3h** (50%)	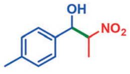 **3i** (78%)
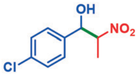 **3g** (82%)	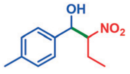 **3k** (70%)	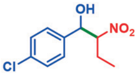 **3l** (72%)	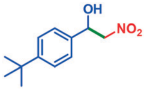 **3m** (85%)
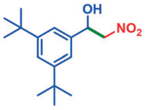 **3n** (82%)	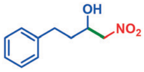 **3o** (91%)	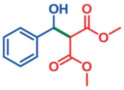 **3p** (55%)	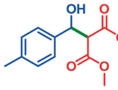 **3q** (50%)
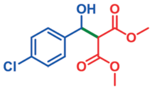 **3r** (58%)	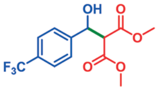 **3s** (69%)	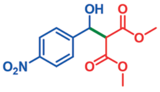 **3t** (78%)	

[a] Reaction conditions: **1** (0.5 mmol), **2** (5 mmol), $^iPr_2EtN$ (20% mol) and MOF catalyst PCN-56-UM (5% mol) in 0.5 mL THF at room temperature with stirring for 24 h. Yields were determined by ^{1}H NMR.

yield after 5 run, Fig. S8†). Besides, PXRD measurements of recycled PCN-56-UM after catalysis revealed that its crystalline framework structure was well preserved, mainly thanks to the robust UiO framework.

The substrate scope of PCN-56-UM catalysed reactions was further examined to explore its broad applications. As shown in Table 1, most of the products can be obtained in a moderate to good yield. Specifically, aromatic aldehydes with electron-withdrawing groups, such as $-NO_2$ and $-CF_3$, exhibited higher yields than those substituted with electron-donating groups. Moreover, the bulk ^{t}Bu group substituted aldehydes can be readily performed this reaction (**3m** and **3n** in Table 1), owing to the large open channel in the PCN-56-UM framework. Aliphatic aldehyde was also amenable to this catalysis giving the expected product **3o** in excellent yield. In addition, we utilized dimethyl malonate as other nucleophilic species to react with benzaldehydes, giving a good yield (**3p**–**3t**).

In summary, we have demonstrated that a urea-based HBD organocatalyst can be readily incorporated into a mixed-strut UiO-68 framework by using a microwave-assisted solvothermal reaction. Because the unwanted self-aggregation of the urea moiety has been prohibited in frameworks, the resulting mixed-strut MOF displays an enhanced catalytic activity toward the Henry reaction in comparison to its homogeneous urea counterpart. In contrast to its pure-strut analogue, the mixed-strut MOF features a robust framework and large open pores, thus, allowing accommodation of large substrates. Further studies of the incorporation of chiral HBD catalysts into MOFs and their application in asymmetric reactions are ongoing.

Conflicts of interest

There are no conflicts to declare.

Acknowledgements

This research is supported by the Natural Science Foundation of Jiangsu Province and Xuzhou City (Grant No. BK20181001, KH17025), the National Natural Science Foundation of China (Grant No. 21702213 and 21302072), TAPP and PAPD of Jiangsu Higher Education Institutions.

Notes and references

1 P. Chauhan, S. Mahajan, U. Kaya, D. Hack and D. Enders, *Adv. Synth. Catal.*, 2015, **357**, 253–281.
2 T. J. Auvil, A. G. Schafer and A. E. Mattson, *Eur. J. Org. Chem.*, 2014, **2014**, 2633–2646.
3 M. S. Taylor and E. N. Jacobsen, *Angew. Chem., Int. Ed.*, 2006, **45**, 1520–1543.
4 C. Min and D. Seidel, *Chem. Soc. Rev.*, 2017, **46**, 5889–5902.
5 Y. Takemoto, *Chem. Pharm. Bull.*, 2010, **58**, 593–601.
6 C. Yang, J. Wang, Y. Liu, X. Ni, X. Li and J.-P. Cheng, *Chem. – Eur. J.*, 2017, **23**, 5488–5497.

7 P. Howlader, P. Das, E. Zangrando and P. S. Mukherjee, *J. Am. Chem. Soc.*, 2016, **138**, 1668–1676.

8 A. Wittkopp and P. R. Schreiner, *Chem. – Eur. J.*, 2003, **9**, 407–414.

9 Y. Qian, G. Ma, A. Lv, H.-L. Zhu, J. Zhao and V. H. Rawal, *Chem. Commun.*, 2010, **46**, 3004–3006.

10 M. Raynal, P. Ballester, A. Vidal-Ferran and P. W. N. M. van Leeuwen, *Chem. Soc. Rev.*, 2014, **43**, 1660–1733.

11 P. R. Schreiner, *Chem. Soc. Rev.*, 2003, **32**, 289–296.

12 V. Simic, L. Bouteiller and M. Jalabert, *J. Am. Chem. Soc.*, 2003, **125**, 13148–13154.

13 F. Lortie, S. Boileau and L. Bouteiller, *Chem. – Eur. J.*, 2003, **9**, 3008–3014.

14 S. J. Connon, *Chem. – Eur. J.*, 2006, **12**, 5418–5427.

15 J. Liang, Z. Liang, R. Zou and Y. Zhao, *Adv. Mater.*, 2017, **29**, 1701139.

16 L. Tuchman-Shukron and M. Portnoy, *Adv. Synth. Catal.*, 2009, **351**, 541–546.

17 P. Borah, J. Mondal and Y. Zhao, *J. Catal.*, 2015, **330**, 129–134.

18 J. M. Roberts, B. M. Fini, A. A. Sarjeant, O. K. Farha, J. T. Hupp and K. A. Scheidt, *J. Am. Chem. Soc.*, 2012, **134**, 3334–3337.

19 H.-C. Zhou and S. Kitagawa, *Chem. Soc. Rev.*, 2014, **43**, 5415–5418.

20 H. Furukawa, K. E. Cordova, M. O'Keeffe and O. M. Yaghi, *Science*, 2013, **341**, 1230444.

21 Y. Cui, B. Li, H. He, W. Zhou, B. Chen and G. Qian, *Acc. Chem. Res.*, 2016, **49**, 483–493.

22 B. Li, H.-M. Wen, Y. Cui, W. Zhou, G. Qian and B. Chen, *Adv. Mater.*, 2016, **28**, 8819–8860.

23 J. Liu, L. Chen, H. Cui, J. Zhang, L. Zhang and C.-Y. Su, *Chem. Soc. Rev.*, 2014, **43**, 6011–6061.

24 L. Jiao, Y. Wang, H.-L. Jiang and Q. Xu, *Adv. Mater.*, 2018, **30**, 1703663.

25 T. Zhang and W. Lin, *Chem. Soc. Rev.*, 2014, **43**, 5982–5993.

26 C. Wang, D. Liu and W. Lin, *J. Am. Chem. Soc.*, 2013, **135**, 13222–13234.

27 B. Li, M. Chrzanowski, Y. Zhang and S. Ma, *Coord. Chem. Rev.*, 2016, **307**, 106–129.

28 C.-D. Wu and M. Zhao, *Adv. Mater.*, 2017, **29**, 1605446.

29 I. Nath, J. Chakraborty and F. Verpoort, *Chem. Soc. Rev.*, 2016, **45**, 4127–4170.

30 P.-Z. Li, X.-J. Wang and Y. Zhao, *Coord. Chem. Rev.*, 2019, **380**, 484–518.

31 J.-S. Qin, S. Yuan, C. Lollar, J. Pang, A. Alsalme and H.-C. Zhou, *Chem. Commun.*, 2018, **54**, 4231–4249.

32 X.-P. Wang, W.-M. Chen, H. Qi, X.-Y. Li, C. Rajnák, Z.-Y. Feng, M. Kurmoo, R. Boča, C.-J. Jia, C.-H. Tung and D. Sun, *Chem. – Eur. J.*, 2017, **23**, 7990–7996.

33 W.-M. Chen, X.-L. Meng, G.-L. Zhuang, Z. Wang, M. Kurmoo, Q.-Q. Zhao, X.-P. Wang, B. Shan, C.-H. Tung and D. Sun, *J. Mater. Chem. A*, 2017, **5**, 13079–13085.

34 Z. Xu, L.-L. Han, G.-L. Zhuang, J. Bai and D. Sun, *Inorg. Chem.*, 2015, **54**, 4737–4743.

35 J. V. Alegre-Requena, E. Marqués-López, R. P. Herrera and D. D. Díaz, *CrystEngComm*, 2016, **18**, 3985–3995.

36 X.-W. Dong, T. Liu, Y.-Z. Hu, X.-Y. Liu and C.-M. Che, *Chem. Commun.*, 2013, **49**, 7681–7683.

37 P. W. Siu, Z. J. Brown, O. K. Farha, J. T. Hupp and K. A. Scheidt, *Chem. Commun.*, 2013, **49**, 10920–10922.

38 Y. Luan, N. Zheng, Y. Qi, J. Tang and G. Wang, *Catal. Sci. Technol.*, 2014, **4**, 925–929.

39 X.-J. Wang, J. Li, Q.-Y. Li, P.-Z. Li, H. Lu, Q. Lao, R. Ni, Y. Shi and Y. Zhao, *CrystEngComm*, 2015, **17**, 4632–4636.

40 A. A. Tehrani, S. Abedi, A. Morsali, J. Wang and P. C. Junk, *J. Mater. Chem. A*, 2015, **3**, 20408–20415.

41 C. M. McGuirk, M. J. Katz, C. L. Stern, A. A. Sarjeant, J. T. Hupp, O. K. Farha and C. A. Mirkin, *J. Am. Chem. Soc.*, 2015, **137**, 919–925.

42 Z. Ju, S. Yan and D. Yuan, *Chem. Mater.*, 2016, **28**, 2000–2010.

43 E. A. Hall, L. R. Redfern, M. H. Wang and K. A. Scheidt, *ACS Catal.*, 2016, **6**, 3248–3252.

44 X. Zhang, Z. Zhang, J. Boissonnault and S. M. Cohen, *Chem. Commun.*, 2016, **52**, 8585–8588.

45 L. Yang, L. Zhao, Z. Zhou, C. He, H. Sun and C. Duan, *Dalton Trans.*, 2017, **46**, 4086–4092.

46 P. C. Rao and S. Mandal, *ChemCatChem*, 2017, **9**, 1172–1176.

47 C. Zhu, Q. Mao, D. Li, C. Li, Y. Zhou, X. Wu, Y. Luo and Y. Li, *Catal. Commun.*, 2018, **104**, 123–127.

48 N. A. Khan and S. H. Jhung, *Coord. Chem. Rev.*, 2015, **285**, 11–23.

49 I. Thomas-Hillman, A. Laybourn, C. Dodds and S. W. Kingman, *J. Mater. Chem. A*, 2018, **6**, 11564–11581.

50 R. Vakili, S. Xu, N. Al-Janabi, P. Gorgojo, S. M. Holmes and X. Fan, *Microporous Mesoporous Mater.*, 2018, **260**, 45–53.

51 Z. Ni and R. I. Masel, *J. Am. Chem. Soc.*, 2006, **128**, 12394–12395.

52 Y. Bai, Y. Dou, L.-H. Xie, W. Rutledge, J.-R. Li and H.-C. Zhou, *Chem. Soc. Rev.*, 2016, **45**, 2327–2367.

53 S. Yuan, L. Feng, K. Wang, J. Pang, M. Bosch, C. Lollar, Y. Sun, J. Qin, X. Yang, P. Zhang, Q. Wang, L. Zou, Y. Zhang, L. Zhang, Y. Fang, J. Li and H.-C. Zhou, *Adv. Mater.*, 2018, **30**, 1704303.

54 J. H. Cavka, S. Jakobsen, U. Olsbye, N. Guillou, C. Lamberti, S. Bordiga and K. P. Lillerud, *J. Am. Chem. Soc.*, 2008, **130**, 13850–13851.

55 A. Schaate, P. Roy, A. Godt, J. Lippke, F. Waltz, M. Wiebcke and P. Behrens, *Chem. – Eur. J.*, 2011, **17**, 6643–6651.

56 W.-Q. Zhang, K. Cheng, H. Zhang, Q.-Y. Li, Z. Ma, Z. Wang, J. Sheng, Y. Li, X. Zhao and X.-J. Wang, *Inorg. Chem.*, 2018, **57**, 4230–4233.

57 Q.-Y. Li, Z. Ma, W.-Q. Zhang, J.-L. Xu, W. Wei, H. Lu, X. Zhao and X.-J. Wang, *Chem. Commun.*, 2016, **52**, 11284–11287.

58 C. Tan, X. Han, Z. Li, Y. Liu and Y. Cui, *J. Am. Chem. Soc.*, 2018, **140**, 16229–16236.

59 H.-L. Jiang, D. Feng, T.-F. Liu, J.-R. Li and H.-C. Zhou, *J. Am. Chem. Soc.*, 2012, **134**, 14690–14693.

60 Z. Hu, A. Gami, Y. Wang and D. Zhao, *Adv. Sustainable Syst.*, 2017, **1**, 1700092.